

Displaced dynamics of binary mixtures in linear and nonlinear optical lattices

Golam Ali Sekh, Mario Salerno

Dipartimento di Fisica "E. R. Caianiello", via ponte don Melillo I-84084, Fisciano (SA), Italy

Aparna Saha, and Benoy Talukdar

Department of Physics, Visva-Bharati University, Santiniketan 731 235, India

(Dated: November 20, 2018)

The dynamical behavior of matter wave solitons of two-component Bose-Einstein condensates (BEC) in combined linear and nonlinear optical lattices (OLs) is investigated. In particular, the dependence of the frequency of the oscillating dynamics resulting from initially slightly displaced components is investigated both analytically, by means of a variational effective potential approach for the reduced collective coordinate dynamics of the soliton, and numerically, by direct integrations of the mean field equations of the BEC mixture. We show that for small initial displacements binary solitons can be viewed as point masses connected by elastic springs of strengths related to the amplitude of the OL and to the intra and inter-species interactions. Analytical expressions of symmetric and anti-symmetric mode frequencies, are derived and occurrence of beatings phenomena in the displaced dynamics is predicted. These expressions are shown to give a very good estimation of the oscillation frequencies for different values of the intra-species interatomic scattering length, as confirmed by direct numerical integrations of the mean field Gross-Pitaevskii equations (GPE) of the mixture. The possibility to use displaced dynamics for indirect measurements of BEC mixture characteristics such as number of atoms and interatomic interactions is also suggested.

PACS numbers: 03.75.-b, 67.85.Hj, 05.45.Yv

I. INTRODUCTION

Binary mixtures of Bose-Einstein condensates (BECs) are presently attracting a great deal of interest in connection with a series of interesting phenomena such as the formation of segregate domains [1], polarized states [2], spin textures [3], topological excitations [4], novel Josephson oscillations [5, 6] Rabi Josephson oscillations [7], four wave mixing [8], etc. Moreover, multi-component BECs have been shown to support nonlinear waves of novel type such as symbiotic solitons [9], domain-wall solitons [10] and combinations of dark-dark [11] and bright-dark solitons [12, 13], the last one leading to long lived oscillations which were experimentally observed in [14]. The possibility to trap binary mixtures in optical lattices (OLs), experimentally demonstrated in [15], has added further interest to the field. In particular, the interplay between the nonlinearity induced by the interatomic interactions and the strength of the OL has been shown to lead to interesting phenomena such as Landau-Zener tunneling [16], transitions from superfluids to Mott insulators [17]. Moreover, existence of nonlinear periodic waves on nonzero backgrounds [18], gap solitons [19], mixed-symmetry modes and breathers both in continuous and discrete (arrays) mixtures [20].

Besides usual (e.g. linear) OLs, it is also possible to introduce a periodic structure in the system by modulating the scattering lengths in space by means of the Feshbach resonance technique [21]. This allows to create what is known as a *nonlinear optical lattice* (NOL). BEC mixtures in NOLs have been recently considered in connection with quantum simulation of novel Hubbard models [22] and interesting phenomena such as sonic analogues

of black holes [23] and control of soliton creation [24]. A possibility of observing delocalizing transition even in one-dimensional BECs loaded in OLs due to the presence of the NOL has been also suggested [25]. For a fresh review on BECs in nonlinear optical lattices we refer the article in [26]. In all these studies, however, the effects of a combined linear and nonlinear optical lattice on the soliton dynamics and the link between dynamical behaviors and interactions, have been scarcely investigated.

The aim of the present paper is to study the mean field dynamics of initially displaced soliton components of binary BEC mixtures in the presence of a combined linear and nonlinear OL. In particular, the dependence of the frequency of the resulting oscillating dynamics on the inter-species interaction and on the number of atoms is investigated. This is done both analytically, by means of a variational effective potential for the displaced dynamics, and numerically by direct integrations of the mean field equations of the BEC mixture. We show that in the limit of small initial displacements, the effective potential leads to a mechanical interpretation of a binary soliton motion in terms of two point masses connected by elastic springs of strengths related to OL's amplitude and to the intra and inter-species interactions. The displaced dynamics, being the same as the one of coupled harmonic oscillators, can be decomposed in term of a normal mode analysis from which analytical expressions of the symmetric and anti-symmetric mode frequencies, are explicitly derived. These expressions are shown to give a very good estimation of the oscillation frequencies for different values of the intra-species interatomic scattering length, as confirmed by direct numerical integrations of the mean field Gross-Pitaevskii equations (GPE) of

the mixture. The occurrence of beating phenomena for unequal and for equal numbers of atoms in the mixture for small interspecies interactions, is also discussed. The stabilities of stationary and oscillating dynamics are investigated by Vakhitov-Kolokolov (VK) criterion [27] and by numerical simulations, respectively. These results suggest the possibility to use dynamical behaviors of suitably prepared initial multi-component BEC solitons as a tool for extracting information about physical characteristics of BEC mixtures such as interatomic interactions and species populations.

The paper is organized as follows. In Sec. II we introduce the mean field model equations describing BEC mixtures in combined linear and nonlinear optical lattices and derive a variational effective potential formulation for the matter waves soliton dynamics. In section III we consider the displaced binary soliton dynamics in the framework of a coupled harmonic oscillator model which is valid in the limit of small initial displacements. Analytical expressions for the symmetric and antisymmetric mode frequencies are explicitly derived. In Sec. IV results of displaced soliton dynamics obtained by direct numerical integrations of the GPE are compared with the analytical predictions. The stability of stationary two component solitons and their slightly displaced dynamics are also investigated. Finally, in Sec. V the main results of the paper are briefly summarized.

II. MODEL EQUATION AND VARIATIONAL ANALYSIS

We consider as a mean field model for a mixture of two homonuclear condensates [28] in an external trapping potential, the following system of coupled Gross-Pitaevskii equations

$$i\hbar \frac{\partial \phi_j}{\partial t} = -\frac{\hbar^2}{2m} \frac{\partial^2 \phi_j}{\partial x^2} + V_{ext}(x) \phi_j + 2\hbar\omega_{\perp} a_s^{(1)} |\phi_j|^2 \phi_j + 2\hbar\omega_{\perp} a_s^{(12)} |\phi_{3-j}|^2 \phi_j. \quad (1)$$

where ϕ_j ($j = 1, 2$) denote the wave function of the binary mixture and $V_{ext}(x)$ the external potential resulting from harmonic and optical lattice confinement, in the following taken of the form

$$V_{ext}(x) = \frac{1}{2} m \omega_x^2 x^2 + V_L \cos(2k_L x). \quad (2)$$

Here ω_x and ω_{\perp} are the longitudinal and transverse trapping frequencies of the harmonic confinement, $a_s^{(1)}$ and $a_s^{(12)}$ are the intra- and inter-species scattering lengths, V_L and k_L are respectively strength and wave number of the optical lattice. Since the longitudinal harmonic confinement introduces only slight modifications to the longitudinal periodic potential (in experimental settings ω_x is of the order of a few Hz), it will be ignored in the following [29]. Introducing dimensionless variables:

$$\tau = t \frac{\hbar}{E_r}, \quad E_r = \frac{\hbar^2 k_L^2}{2m}, \quad s = x k_L \quad \text{and} \quad \psi_j = \frac{\phi_j}{\sqrt{k_L}} \quad (3)$$

Eqs. 1 can be written in the form

$$i \frac{\partial \psi_j}{\partial \tau} = -\frac{1}{2} \frac{\partial^2 \psi_j}{\partial s^2} + V_0 \cos(2s) \psi_j + g_{11} |\psi_j|^2 \psi_j + g_{12} |\psi_{3-j}|^2 \psi_j \quad (4)$$

where $V_0 = \frac{V_L}{E_r}$ and $g_{11} = 2a_s^{(1)} k_L$ and $g_{12} = 2a_s^{(12)} k_L$ are rescaled intra- and inter-species interaction strengths. In this Eqs. the order parameter ψ_j is normalized to the total number of atoms such that $\int_{-\infty}^{+\infty} (|\psi_1|^2 + |\psi_2|^2) ds = N_1 + N_2$, where N_j , $j = 1, 2$ are the separately conserved numbers of atoms in each component. In the following we fix $k_L = 2$ and assume a dependence of the intra-species interaction of the form

$$g_{11} = g_{11}^{(0)} + g_{11}^{(1)} \cos(2s) \quad (5)$$

with the spatial modulation part denoting a NOL of strength $g_{11}^{(1)}$. In an experimental context such a spatial modulation could be produced by optically induced Feshbach resonances [30] e.g. by a laser field tuned near a photo association transition. Virtual radiative transitions of a pair of interacting atoms to this level can then change the value and even reverse the sign of the scattering length. It can be shown that a modulation of the laser field intensity of the form $I = I_0 \cos^2(\kappa x)$ reflects in a modulation of the scattering length of the form $a_s^{(1)}(x) = a_{s0}^{(1)} [1 + \alpha I / (\delta + I)]$, where $a_{s0}^{(1)}$ is the intra-species scattering length in the absence of light, δ is the frequency detuning of the light from the resonance, and α is a constant factor [30, 31]. For weak intensities $I_0 \ll |\delta|$ the real part of the scattering length can be then approximated as $a_s^{(1)} = a_{s0}^{(1)} + a_{s1}^{(1)} \cos^2(\kappa x)$ which is essentially the same form assumed in Eq. (5).

Note that in the absence of the OLs and with $g_{12} = 0$, Eq. (4) decouple into two nonlinear Schrödinger equations which admit, for attractive intra-species interactions, exact bright soliton solutions with typical Gaussian-like function shape. With the view to solve Eqs. in (4) within a variational approach, we then adopt for the coupled soliton wavefunction the following ansatz

$$\psi_j(s, \tau) = A_j \exp\left[-\frac{(s - s_{0j})^2}{2a_j^2} + i(\dot{s}_{0j}(s - s_{0j}) + \Phi_j)\right], \quad j = 1, 2 \quad (6)$$

with parameters A_j , a_j , s_{0j} , Φ_j , denoting amplitude, width, center of mass and phase of the soliton, respectively, taken in the following as time-dependent parameters. Note that the wavefunction is normalized to the total number of atoms N_j so that $A_j = \sqrt{\frac{N_j}{\pi a_j}}$.

The effective Lagrangian for the system is written as $\langle \mathcal{L} \rangle = \int_{-\infty}^{\infty} L ds$ with the Lagrangian density L given by

$$\langle L \rangle = \sum_{j=1}^2 \sqrt{\pi} a_j A_j^2 \left[\frac{1}{4a_j^2} + \frac{g_{11}^{(0)}}{2\sqrt{2}} A_j^2 + V_0 e^{-a_j^2} \cos(2s_{0j}) \right]$$

$$\begin{aligned}
& + \frac{g_{11}^{(1)}}{2\sqrt{2}} e^{-a_j^2/2} A_j^2 \cos(2s_{0j}) - \frac{1}{2} \dot{s}_{0j}^2 + \dot{\Phi}_j \Big] \\
& + g_{12} a_1 a_2 A_1^2 A_2^2 \frac{\exp[-\frac{(s_{01}-s_{02})^2}{a_1^2+a_2^2}]}{\sqrt{a_1^2+a_2^2}}. \quad (7)
\end{aligned}$$

From the Ritz optimization conditions [32], we have $\frac{\delta \langle \mathcal{L} \rangle}{\delta \Phi_j} = 0$, $\frac{\delta \langle \mathcal{L} \rangle}{\delta A_j} = 0$, $\frac{\delta \langle \mathcal{L} \rangle}{\delta a_j} = 0$ and $\frac{\delta \langle \mathcal{L} \rangle}{\delta s_{0j}} = 0$. The first optimization condition

$$\frac{d}{d\tau} [\sqrt{\pi} a_j A_j^2] = 0, \quad (8)$$

in conjunction with the normalization condition of ψ_j implies that $\sqrt{\pi} a_j A_j^2 = N_j$ is a constant. This constrain when used in the relations obtained from the other optimization conditions give

$$\begin{aligned}
& \frac{1}{2a_j^2} + g_{11}^{(0)} \sqrt{\frac{2}{\pi}} \frac{N_j}{a_j} + 2V_0 e^{-a_j^2} \cos(2s_{0j}) - \dot{s}_{0j}^2 + 2\dot{\Phi}_j \\
& + g_{11}^{(1)} \sqrt{\frac{2}{\pi}} N_j e^{-\frac{a_j^2}{2}} \cos(2s_{0j}) \\
& + \frac{2g_{12}}{\sqrt{\pi}} N_{3-j} \frac{\exp[-\frac{(s_{01}-s_{02})^2}{a_1^2+a_2^2}]}{\sqrt{a_1^2+a_2^2}} = 0, \quad (9)
\end{aligned}$$

$$\begin{aligned}
& - \frac{1}{2a_j^3} + \frac{g_{11}^{(0)}}{\sqrt{2\pi}} \frac{N_j}{a_j^2} + \frac{2V_0}{a_j} (1 - 2a_j^2) e^{-a_j^2} \cos(2s_{0j}) \\
& + \frac{g_{11}^{(1)} N_j}{\sqrt{2\pi} a_j^2} (1 - a_j^2) e^{-a_j^2/2} \cos(2s_{0j}) - \frac{\dot{s}_{01}}{a_1^2} + \frac{2\dot{\Phi}_1}{a_j} \\
& + \frac{g_{12} N_{3-j}}{\sqrt{\pi} a_j} [a_{3-j}^4 + a_j^2 a_{3-j}^2 + 2a_j^2 (s_{01} - s_{02})^2] \\
& \times \frac{e^{-\frac{(s_{01}-s_{02})^2}{a_1^2+a_2^2}}}{(a_1^2+a_2^2)^{5/2}} \quad (10)
\end{aligned}$$

and

$$\begin{aligned}
& \ddot{s}_{0j} - 2V_0 e^{-a_j^2} \sin(2s_{0j}) - \frac{g_{11}^{(1)} N_j e^{-a_j^2/2}}{\sqrt{2\pi} a_j} \sin(2s_{0j}) \\
& + (-1)^j \frac{2g_{12} N_{3-j} (s_{01} - s_{02})}{\sqrt{\pi} (a_1^2 + a_2^2)^{3/2}} e^{-\frac{(s_{01}-s_{02})^2}{a_1^2+a_2^2}} = 0. \quad (11)
\end{aligned}$$

In order to derive an explicit formula for the effective interacting potential of the coupled solitons, we consider that the condensates are symmetrically placed with respect to the a OL minimum i.e, $s_{0j} = \pm s_0/2$. In this case, Eqs. in (11) can be combined to give

$$\begin{aligned}
& \ddot{s}_0 - 2V_0 (e^{-a_1^2} + e^{-a_2^2}) \sin(s_0) \\
& - \frac{2g_{12}(N_1 + N_2)s_0}{\sqrt{\pi}(a_1^2 + a_2^2)^{3/2}} e^{-\frac{s_0^2}{a_1^2+a_2^2}} \\
& - \frac{g_{11}^{(1)}}{\sqrt{2\pi}} \left(\frac{N_1}{a_1} e^{-a_1^2/2} + \frac{N_2}{a_2} e^{-a_2^2/2} \right) \sin(s_0) = 0 \quad (12)
\end{aligned}$$

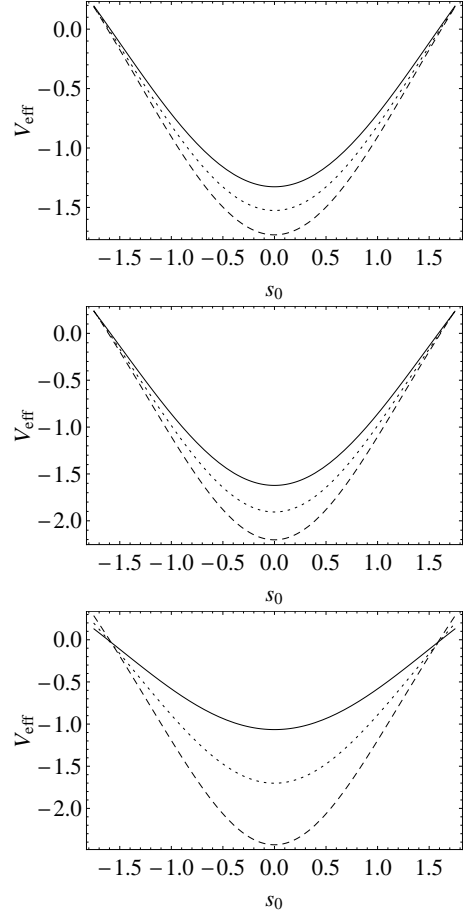


FIG. 1: Effective potential versus separation for $V_0 = -0.5$. Top panel gives V_{eff} with $N_1 = 1.0$ and $N_2 = 0.5$ for different values of g_{12} , namely, -0.2 (solid), -0.4 (dotted) and -0.6 (dashed). The middle panel gives V_{eff} with $N_1 = 1.0$ and $N_2 = 1.0$ for different values of g_{12} , namely, -0.2 (solid), -0.4 (dotted) and -0.6 (dashed). The bottom panel shows V_{eff} with $g_{12} = -0.5$ for different values of $N = N_1 = N_2$, namely, $N = 0.4$ (solid), 0.8 (dotted) and 1.2 (dashed).

as the evolution equation for the separation s_0 between center of the solitons. Notice that Eq. (12) is the same as the dynamics of a Newtonian particle in the effective potential

$$\begin{aligned}
V_{\text{eff}}(s_0) = & \left[2V_0 (e^{-a_1^2} + e^{-a_2^2}) \cos(s_0) \right. \\
& + \frac{g_{11}^{(1)}}{\sqrt{2\pi}} \left(\frac{N_1}{a_1} e^{-a_1^2/2} + \frac{N_2}{a_2} e^{-a_2^2/2} \right) \cos(s_0) \\
& \left. + \frac{g_{12}(N_1 + N_2)}{\sqrt{\pi}(a_1^2 + a_2^2)^{1/2}} e^{-\frac{s_0^2}{a_1^2+a_2^2}} \right]. \quad (13)
\end{aligned}$$

Also notice that this potential has the absolute minimum in the origin and that for small values of s_0 around the minimum of the potential can be approximated as a harmonic potential. In such approximations, the small oscillation frequency of displaced solitons dynamics can

be written as

$$\omega = \left[-2V_0(e^{-a_1^2} + e^{-a_2^2}) - \frac{2g_{12}(N_1 + N_2)}{(a_1^2 + a_2^2)^{3/2}\sqrt{\pi}} - \frac{g_{11}^{(1)}}{\sqrt{2\pi}} \left(\frac{N_1}{a_1} e^{-a_1^2/2} + \frac{N_2}{a_2} e^{-a_2^2/2} \right) \right]^{1/2}. \quad (14)$$

Moreover, one can show that the vanishing condition of $\frac{\delta \langle \mathcal{L} \rangle}{\delta A_j}$ gives the chemical potential, μ , of stationary components as:

$$\mu_j = \frac{1}{4a_j^2} + \frac{g_{11}^{(0)} N_j}{a_j \sqrt{2\pi}} + \frac{g_{11}^{(1)} N_j}{a_j \sqrt{2\pi}} e^{-a_j^2/2} \cos(s_0) + V_0 e^{-a_j^2} \cos(s_0) + \frac{g_{12} N_{3-j}}{\sqrt{\pi}} \frac{e^{-\frac{s_0^2}{a_1^2 + a_2^2}}}{\sqrt{a_1^2 + a_2^2}} \quad (15)$$

(in writing Eq. (15) we have used $\Phi_j = -\mu_j \tau$ and $\dot{s}_{0j} = 0$ in Eq. (9)). This expression can be used (see below) to study the stability of stationary two component solitons through the Vakhitov-Kolokolov (VK) criterion. From Eq. (13) we see that the effective potential for the coupled solitons dynamics is highly anharmonic and consists of three terms: the first two arise from the linear and nonlinear optical lattices while the third one comes from the mutual interaction between the solitons. The mutual interaction term depends both on the number of atoms in the condensates and on the strength of the interactions. This part of the potential will therefore change sensitively with the variation of N and g_{12} .

In Fig. 1 we show the effective potential as a function of s_0 for two attractively interacting solitons and different values of $-g_{12}$ (left and middle panels) and $N = N_1 = N_2$ (right panel). More specifically, left panel give V_{eff} with $N_1 = 1$ and $N_2 = 0.5$ while middle panel shows V_{eff} with $N_1 = N_2 = 1$ for different values of $-g_{12}$. Note that the inter-species interaction is effective mainly for BEC components with a significant spatial overlapping e.g. when they are very close to each other. In this situation an oscillatory dynamics of the BEC components around their common center of mass can be started by slightly displacing them from the equilibrium position corresponding to the fundamental minimum of the effective potential in Fig. 1. Also note that for an attractive inter-species interaction the absolute minimum of the effective potential becomes deeper and deeper as $N|g_{12}|$ is increased. Therefore, the reduced equation of motion in (14) implies that the solitons oscillation with respect to each other if they are placed very close to the effective potential minimum at $s_0 = 0$. For repulsive inter-species interactions, however, the effective potential will have the shape of a barrier (rather than a potential well) with a maximum (rather than a minimum) at the origin. In this case, the soliton components move away from each other keeping their shapes unchanged [33].

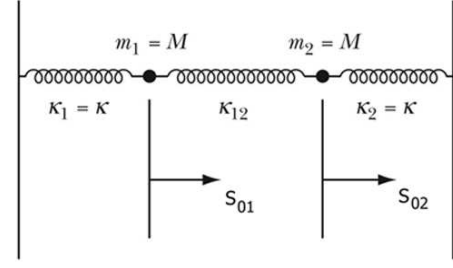


FIG. 2: Mechanical model of displaced binary soliton dynamics in terms of harmonic oscillators of elastic constant κ coupled by a spring of elastic constant κ_{12} .

III. NORMAL MODE ANALYSIS OF DISPLACED BINARY SOLITON DYNAMICS

It is useful to gain some modeling insight of the displaced binary soliton dynamics in the limit of small displacements $s_{01} \ll 1$ and $s_{02} \ll 1$. In this case Eq. (11) reduces to

$$\ddot{s}_{0j} - \left(4V_0 e^{-a_j^2} + \frac{2g_{11}^{(1)} N_j}{\sqrt{2\pi} a_j} e^{-a_j^2/2} + \frac{2g_{12} N_{3-j}}{\sqrt{\pi} (a_1^2 + a_2^2)^{3/2}} \right) s_{0j} + \frac{2g_{12} N_{3-j}}{\sqrt{\pi} (a_1^2 + a_2^2)^{3/2}} s_{03-j} = 0. \quad (16)$$

Let us concentrate for simplicity on binary solitons with equal number of atoms and equal widths e.g. $N_1 = N_2 = N$ and $a_1 = a_2 = a$. Introducing parameters

$$M = \frac{\sqrt{2\pi} a^3}{N}, \quad \kappa_{12} = -g_{12}, \quad (17)$$

$$\kappa = -4V_0 \frac{\sqrt{2\pi} a^3 e^{-a^2}}{N} - 2g_{11}^{(1)} a^2 e^{-a^2/2}, \quad (18)$$

we can rewrite Eq. (16) in the form

$$\ddot{s}_{01} = -\frac{\kappa + \kappa_{12}}{M} s_{01} + \frac{\kappa_{12}}{M} s_{02}, \quad (19)$$

$$\ddot{s}_{02} = -\frac{\kappa + \kappa_{12}}{M} s_{02} + \frac{\kappa_{12}}{M} s_{01}, \quad (20)$$

$$(21)$$

which are the same as the equation of motion of two coupled identical harmonic oscillators of mass M and elastic spring κ connected by a spring of elastic constant κ_{12} (see Fig. 2). In the absence of inter-species interaction, (as it is the case, for example, when the interspecies scattering length is detuned to zero by means of a Feshbach resonance) In the presence of interspecies interactions the above equations are readily decoupled in the normal mode coordinates: $\xi_1 = s_{01} - s_{02}$, $\xi_2 = s_{01} + s_{02}$, this giving $M\ddot{\xi}_i = -\omega_i^2 \xi_i$, $i = 1, 2$, with characteristic frequencies

$$\omega_1 = \pm \sqrt{\frac{\kappa + 2\kappa_{12}}{M}}, \quad \omega_2 = \pm \sqrt{\frac{\kappa}{M}} \quad (22)$$

and explicit normal mode solutions

$$\xi_i(t) = A_i^+ e^{i\omega_i t} + A_i^- e^{-i\omega_i t}, \quad i = 1, 2. \quad (23)$$

The most general solution of the displaced soliton dynamics in the coupled harmonic oscillator approximation follows from Eq. (23) as

$$s_{01}(t) = \frac{1}{2}(\xi_2(t) + \xi_1(t)), \quad s_{02}(t) = \frac{1}{2}(\xi_2(t) - \xi_1(t)). \quad (24)$$

From these equations we see that the solution ξ_1 associated to the frequency $\omega_1 \equiv \omega_{asym}$ corresponds to an asymmetric (out of phase) oscillation of the displaced two component soliton, while the solution ξ_2 corresponds to a symmetric (in phase) motion of frequency $\omega_2 \equiv \omega_{sym}$ in which the coupling spring remains unstretched. Notice that ω_{asym} is the same as the expression of the frequency derived in Eq. (14). Also note that in analogy with optical and acoustical vibrations of molecules, this frequency, for attractive inter- and intra-species interactions, is always higher than the frequency ω_{sym} of the symmetric mode, e.g. $\omega_{asym}/\omega_{sym} \geq 1$, with the equality holding in the case $g_{12} = 0$. More explicitly, the following dependence for the frequency ratio of asymmetric and symmetric modes on parameters of the binary mixture, is derived:

$$\begin{aligned} \nu_r &\equiv \frac{\omega_{asym}}{\omega_{sym}} \\ &= \left[1 + \frac{Ng_{12}e^{a^2/2}/a^2}{2V_0\sqrt{2\pi}ae^{-a^2/2} + Ng_{11}^{(1)}} \right]^{1/2}. \end{aligned} \quad (25)$$

Note that in the weak coupling limit $|g_{12}| \ll 1$ the displaced dynamics will display typical beating phenomena with a high frequency component oscillating inside a slowly varying envelope, with beating frequencies $\omega_{beat} = \omega_{asym} - \omega_{sym}$, plus order combinations.

For the general case $N_1 \neq N_2$ (equivalently, $a_1 \neq a_2$), the dependence of characteristic frequencies of the oscillators on parameters can be derived in similar manner. In the next section we shall compare the above predictions for the soliton displaced dynamics with direct numerical integrations of the coupled GPE in (4).

IV. DYNAMICS AND STABILITY OF DISPLACED BINARY SOLITONS: NUMERICAL RESULTS

In the following coupled GPE numerical investigations we assume that solitons prepared in such a manner that their relative coordinates are located at small distances from the minimum of V_{eff} in Fig. 1. We remark that initial small displacements of the two components of the mixture could be experimentally induced by a rapid change of the inter-species scattering length from negative to positive and then to negative again, by means of the Feshbach resonance technique. The inversion of the

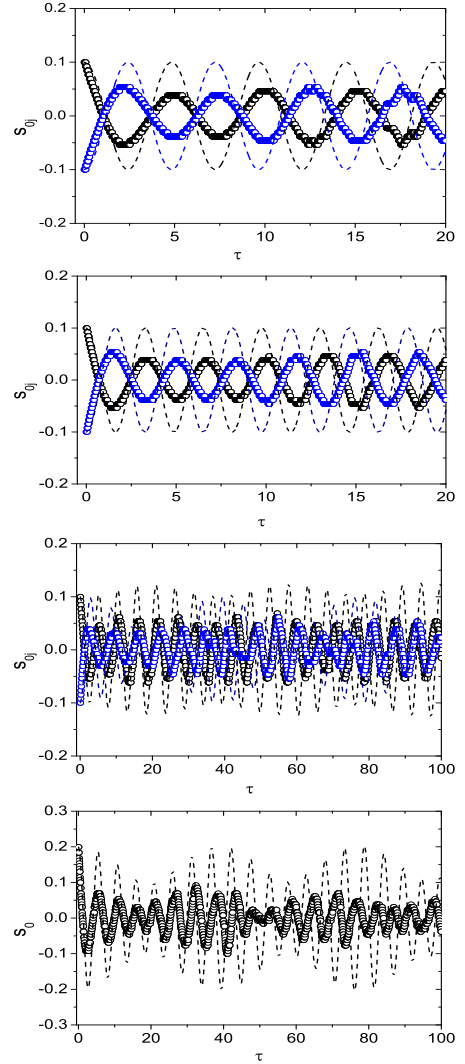


FIG. 3: Oscillation of coupled BEC components for $V_0 = -0.5$, $g_{11}^{(0)} = -1$, $g_{11}^{(1)} = -0.5$ and $s_0 = 0.2$. Here, number of panels is counted from the top. First panel shows motion of soliton profiles for $N_1 = N_2 = 1.0$ and $g_{12} = -0.2$. Second panel. Same as in first panel but for $N_1 = N_2 = 1.4$ and $g_{12} = -0.5$. Third panel. Motion of the centers of soliton components for unequal number of atoms $N_1 = 1$, $N_2 = 0.5$ and for $g_{12} = -0.2$. The bottom panel show beatings arising from the superposition of the oscillatory components displayed in the 3rd panel. In all panels curves with big circles give results for PDEs in (4) while dashed curves represent results for ODEs in (11).

sign of the interaction for a small fraction of time can be achieved with a properly designed time-dependent external magnetic field. The component solitons will move in opposite directions during the short repulsive inter-species interaction time, and will become slightly separated (separation can be made small by properly reducing the repulsive time). Taking into account detectable length scales of real experiments[34], we use in most of the calculations $s_0 = 0.2$, although larger initial displacements ($s_0 \approx 1$) will also be used for anharmonic effects.

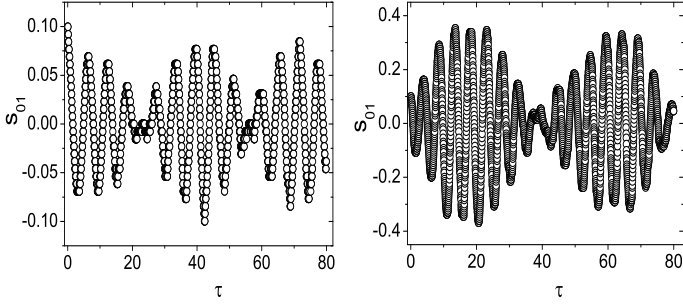


FIG. 4: Beating dynamics of displaced binary BEC solitons with an equal number of atoms $N_1 = N_2 = 1$, for $g_{12} = -0.2$, $s_{01} = 0.1$, $s_{02} = 1.3$ (left panel) and $g_{12} = -0.5$, $s_{01} = 0.1$, $s_{02} = -1.3$ (right panel). Other parameters are fixed as $g_{11}^{(0)} = -1$, $g_{11}^{(1)} = -0.5$, $V_0 = -0.5$.

In Fig. 3 we show typical dynamics of displaced binary solitons arising from a symmetric initial displacements with respect to the effective potential minimum. The top two panels refers to the case of unequal numbers of atoms. We see that in this case the soliton components oscillate with the same frequency which depends on inter-species interaction strength and on number of atoms in the condensates (compare 1st and 2nd panel). For $N_1 \neq N_2$, however, the oscillation frequencies of each component become unequal (3rd panel) with appearance of well-known beating phenomenon. The general solution in Eq. (24) shows that the beating phenomena is expected also for equal number of atoms and small inter-species interactions if the motion is started with a generic initial displacement $|s_{01}| \neq |s_{02}|$. This is exactly what the PDE calculations in Fig. 4 show for the case $N_1 = N_2 = 1$ and $|s_{01}| \neq |s_{02}|$, in agreement with our normal mode analysis.

The dependence of oscillation frequency (ν) on g_{12} is depicted in Fig. 5 for the case $N_1/N_2 = 1$. In particular, the top left panel of this figure shows ν vs $-g_{12}$ for closely spaced solitons ($s_{0j} = \pm 0.1$) while the top right panel gives the dependence on g_{12} for $s_{0j} = \pm 0.5$. Notice that in both cases one can estimate values of ν very close to the exact numerical results (dotted curve) from our simple analytical calculation. It may be pointed out that the variational approach gives little higher values of ν than that of the numerical integration for $s_{0j} = \pm 0.1$ (top panel) while we observed the opposite in the bottom panel. Also note that for overlapped condensates results obtained from analytical formula in (14) and ODEs in (12) are same. However, with the increase of separation deviation between these two results becomes appreciable. The deviation of analytical curve (solid) with ODE calculations (dashed) implies that the effects of anharmonicity has been captured. In addition, the curves in both the panels clearly indicate that the values of ν increase as g_{12} increases. This correlates with the fact that the corresponding effective potentials become more deep and acquire larger curvatures at the origin as these parameters

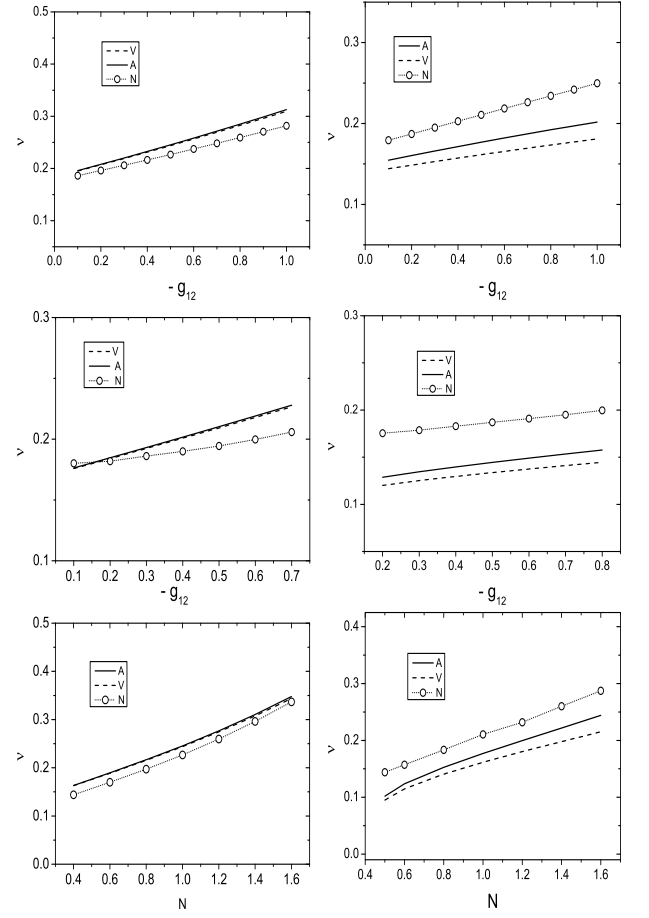


FIG. 5: Top left panel. Frequency of the oscillation of the BEC components vs the inter-species interaction strength for fixed number of atoms $N_1 = N_2 = 1$ and $s_0 = 0.2$. Top right panel: Same as that in the left panel but for a larger initial displacement $s_0 = 1.0$. Middle left panel. Frequency of the oscillation of the BEC components vs the inter-species interaction strength for the case of unequal number of atoms $N_1 = 1$ and $N_2 = 0.5$. and $s_0 = 0.2$. Middle right panel: Same as that in corresponding left panel but for $s_0 = 1.0$. Bottom left panel. Frequency of the oscillation of BEC components versus the number of atoms for fixed inter-species interaction strength $g_{12} = -0.5$ and $s_0 = 0.2$. Bottom right panel. Same as that in the left panel but $s_0 = 1.0$. In all the panels the continuous curve represents the analytical expression in equation (14), the dashed curve stands for result obtained from ODE in (12) and open circles denote numerical GPE calculations. In each case, other parameters are fixed as: $V_0 = -0.5$, $g_{11}^{(0)} = -1$ and $g_{11}^{(1)} = -0.5$

are increased, clearly leading to higher frequency values.

In the middle panel of Fig. 5 we portrayed a plot similar to that in the top panel but with $N_1 \neq N_2$ and observed same behavior of the frequency curve. However, the observed frequency in this case is little smaller than the previous one. This might be associated with the fact that effective inter-species interaction is relatively larger $N_1 = N_2$ than $N_1 \neq N_2$ (Fig. 1). In order to find dependence of ν on number of atoms in the condensates,

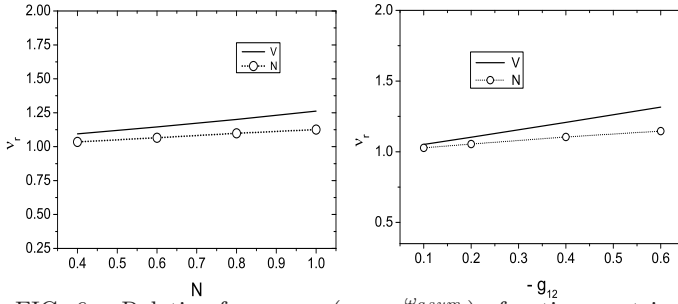


FIG. 6: Relative frequency ($\nu_r = \frac{\omega_{asym}}{\omega_{sym}}$) of antisymmetric and symmetric modes vs number of atoms N (left panel) and inter-species interaction g_{12} (right panel). In both panels the solid curve refers to Eq.(25) while the open dots refer to GPEs numerical integrations. Other parameters are fixed as $V_0 = -0.5, g_{11}^{(0)} = -1, g_{11}^{(1)} = -0.5, s_0 = 0.2$.

we consider only the case $N = N_1 = N_2$ and plot in the bottom panels of Fig. 5 variation of ν with N for $g_{12} = -0.5$. Particularly, the left bottom panel shows ν vs N for $s_0 = 0.2$ while the right bottom panel gives a similar plot but $s_0 = 1.0$. As in the previous case, the frequency of oscillations here also increases with the increase of number of atoms due to the increase of effective inter-species interaction. Notice that the analytical (solid) and/or ODE (dashed) calculations here also gives a very good estimate of ν of the exact numerical calculation (dots with circles). The expected discrepancy of analytical curve from the ODE curve due to anharmonic effect is prominent for $s_0 = 1.0$ (bottom right panel). In Sec. III we showed that the frequency of the asymmetric mode is always greater than that of the symmetric one with a ratio ν_r that depends on both g_{12} and N . In Fig. 6 we compare the dependence of ν_r on g_{12} and on N as obtained from Eq. (25) with the one obtained from PDE calculations. We see that in both cases a relatively good agreement is found. It is also clear, both from analytical and numerical results, that ν_r increases with the increase of either inter-species interaction and number of atoms, and that the analytical results are slightly overestimating this growth.

The stability of the oscillatory soliton dynamics has been checked with slightly perturbed initial BEC profiles for given values of parameters and then allowed them to evolve according the GPE coupled equations. Density plots for the evolution of soliton profiles for different values of g_{12} and number of atoms is displayed in Fig. 7. This figure clearly indicates that during time evolution soliton profiles remain undistorted. To confirm the stable evolution of the density profiles we slightly vary initial conditions and noticed that they still evolve uniformly with time. The stability of soliton profile can also be examined from the phase plot of coupled ordinary differential equations in (11). We have verified that in each case considered by us the phase plot exhibits stable focus.

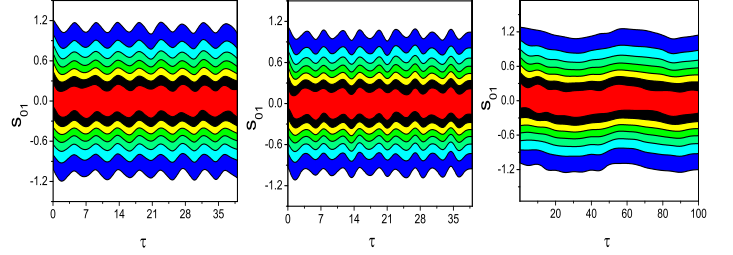


FIG. 7: Time evolution of displaced component binary soliton densities. In each contour plots we have taken slightly perturbed initial conditions for parameter values $V_0 = -0.5, g_{11}^{(0)} = -1, g_{11}^{(1)} = -0.5$. Left and middle panels show density evolution for $N_1 = N_2 = 1$ and $g_{12} = -0.2$ (left panel) and for $N_1 = N_2 = 0.8$ and $g_{12} = -0.5$. Right panel refers to the case of unequal number of atoms $N_1 = 1, N_2 = 0.5$ for $g_{12} = -0.2$.

V. CONCLUSION

In this paper we have studied the dynamics of matter wave solitons of two-component Bose-Einstein condensates in combined linear and nonlinear optical lattices.

In particular, we have investigated the dependence of the oscillating dynamics resulting from two initially displaced BEC soliton components on the inter-species interaction and on the number of atoms. We showed that for small initial displacements binary solitons can be viewed as point masses connected by elastic springs of strengths related to the amplitude of the OL and to the intra and inter-species interactions. The displaced dynamics in can be decomposed in term of normal mode analysis from which analytical expressions of the symmetric and anti-symmetric mode frequencies, are derived. The occurrence of beating phenomena both for unequal and for equal numbers of atoms for small interspecies interactions, was also predicted. The stability of the oscillating dynamics has been also investigated by direct numerical GPE integrations. The predictions of the effective potential approach are found to be in quantitative agreement with direct numerical simulations. These results suggest the possibility to use dynamical behaviors of suitably prepared initial multi-component BEC solitons as a tool for extracting information about physical characteristics of BEC mixtures such as interatomic interactions and species populations. In this respect, we remark that in contrast to intra-species interactions, direct measurements of the inter-species scattering lengths are more difficult to access. The possibility to measure interspecies scattering lengths through dynamical behaviors of displaced BEC components represents therefore an interesting possibility which could be tested in real experiments.

Acknowledgment

GAS wish to thank the Department of Physics of the University of Salerno for the hospitality received and for a one year research grant (AR–2011) during which

this work has been done. MS acknowledges partial support from the Ministero dell’ Istruzione, dell’ Università e della Ricerca (MIUR) through a Programmi di Ricerca Scientifica di Rilevante Interesse Nazionale (PRIN)-2008.

-
- [1] J. Stenger, S. Inouye, D. M. Stamper-Kurn, H. -J. Miesner, A. P. Chikkatur and W. Ketterle, *Nature* (London) **396**, 345(1998); I. M. Merhasin, B. A. Malomed and R. Driben, *J. Phys. B* **38**, 877(2005); S. Tojo, Y. Taguchi, Y. Masuyama, T. Hayashi, H. Saito and T. Hirano, *Phys. Rev. A* **82**, 033609(2010).
 - [2] H. E. Nistazakis, D. J. Frantzeskakis, P. G. Kevrekidis, B. A. Malomed, R. Carretero-Gonzalez and A. R. Bishop, *Phys. Rev. A* **76**, 063603(2007).
 - [3] A. E. Leanhardt, Y. Shin, D. Kielpinski, D. E. Pritchard and W. Ketterle, *Phys. Rev. Lett.* **90**, 140403(2003).
 - [4] R. P. Anderson, C. Ticknor, A. I. Sidorov and B. V. Hall, *Phys. Rev. A* **80**, 023603(2009); S. B. Papp, J. M. Pino and C. E. Wieman, *Phys. Rev. Lett.* **101**, 040402(2008); G. Thalhammer, G. Barontini, L. DeSarlo, J. Catani, F. Minardi and M. Inguscio, *Phys. Rev. Lett.* **100**, 210402(2008)
 - [5] J. Williams, R. Walser, J. Cooper, E. Cornell and M. Holland, *Phys. Rev. A* **59**, R31(1999).
 - [6] G. Mazzaella, M. Moratti, L. Salasnich, M. Salerno and F. Toigo, *J. Phys. B: At. Mol. Opt. Phys.* **42**, 125301(2009).
 - [7] S. Ashhab and C. Lobo, *Phys. Rev. A* **66**, 013609(2002); G. Mazzaella, B. A. Malomed, L. Salasnich, M. Salerno and F. Toigo *J. Phys. B: At. Mol. Opt. Phys.* **44**, 035301(2011).
 - [8] M. Trippenbach, Y. B. Band and P. S. Julienne, *Phys. Rev. A* **62**, 023608(2000).
 - [9] V. M. Perez-Garcia and J. B. Beitia, *Phys. Rev. A* **72**, 033620 (2005); S. K. Adhikari, *Phys. Lett. A* **346**, 179(2005).
 - [10] S. Coen and M. Haelterman, *Phys. Rev. Lett.* **87**, 140401(2001); K. Kasamatsu and M. Tsubota, *Phys. Rev. Lett.* **93**, 100402(2004).
 - [11] A. P. Sheppard and Y. S. Kivshar, *Phys. Rev. E* **55**, 4773(1997).
 - [12] Th. Busch and J. R. Anglin, *Phys. Rev. Lett.* **87**, 010401(2001).
 - [13] D. J. Kaup and B. A. Malomed, *Phys. Rev. A* **48**, 599(1993).
 - [14] C. Becker, S. Stellmer, P. Soltan-Panahi, S. Dorscher, M. Baumert, Richter Eva-Maria, J. Kronjager, K. Bongs and K. Sengstock, *Nat. Phys.* **4**, 496(2008).
 - [15] J. M. Higbie, L. E. Sadler, S. Inouye, A. P. Chikkatur, S. R. Leslie, K. L. Moore, V. Savalli and D. M. Stamper-Kurn, *Phys. Rev. Lett.* **95**, 050401(2005); A. Widera, F. Gerbier, S. Fölling, T. Gericke, O. Mandel and I. Bloch, *Phys. Rev. Lett.* **95**, 190405(2005).
 - [16] Li Guan-Qiang, *Commun. Theor. Phys.* **54**, 101(2010).
 - [17] M. Lewenstein, L. Santos, M. A. Baranov and H. Fehrmann, *Phys. Rev. Lett.* **92**, 050401(2004); I. Bloch, J. Dalibard and W. Zwerger, *Rev. Mod. Phys.* **80**, 885(2008).
 - [18] N. A. Kostov, V. Z. Enolskii, V. S. Gerdjikov, V. V. Konotop and M. Salerno, *Phys. Rev. E* **70**, 056617(2004).
 - [19] E. A. Ostrovskaya and Y. S. Kivshar, *Phys. Rev. Lett.* **92**, 180405(2004).
 - [20] H. A. Cruz, V. A. Brazhnyi, V. V. Konotop, G. L. Alfimov and M. Salerno, *Phys. Rev. A* **76**, 013603(2007).
 - [21] H. Feshbach, *Ann. Phys.(NY)* **5**, 375(1958); S. Inouye, M. R. Andrews, J. Stenger, H. -J. Miesner, D. M. Stamper-Kurn and W. Ketterle, *Nature* **392**, 151(1998); P. O. Fedichev, Yu. Kagan, G. V. Shlyapnikov and J. T. M. Walraven, *Phys. Rev. Lett.* **77**, 2913(1996); M. Theis, G. Thalhammer, K. Winkler, M. Hellwig, G. Ruff, R. Grimm and J. H. Denschlag, *Phys. Rev. Lett.* **93**, 123001(2004).
 - [22] X. L. Deng, D. Porras and J. I. Cirac, *Phys. Rev. A* **77**, 033403(2008).
 - [23] L. J. Garay, J. R. Anglin, J. I. Cirac and P. Zoller, *Phys. Rev. Lett.* **85**, 4643 (2000).
 - [24] M. I. Rodas-Verde, H. Michinel and V. M. Perez-Garcia, *Phys. Rev. Lett.* **95**, 153903(2005).
 - [25] Yu. V. Bludov, V. A. Brazhnyi and V. V. Konotop, *Phys. Rev. A* **76**, 023603(2007).
 - [26] Y. V. Kartashov, B. A. Malomed and L. Torner, *Rev. Mod. Phys.* **83**, 247(2011).
 - [27] N. G. Vakhitov and A. A. Kolokolov, *RadioPhys. Quantum electron.* **16**, 783(1975); A. A. Kolokolov, *ibid* **17**, 283(1986).
 - [28] C. J. Myatt, E. A. Burt, R. W. Ghrist, E. A. Cornell and C. E. Wieman, *Phys. Rev. Lett.* **78**, 586(1997).
 - [29] O. Morsch and M. Oberthaler, *Rev. Mod. Phys.* **78**, 179(2006).
 - [30] P. O. Fedichev, Yu. Kagan, G. V. Shlyapnikov, and J. T. M. Walraven, *Phys. Rev. Lett.* **77**, 2913 (1996).
 - [31] H. Sakaguchi and B. A. Malomed, *Phys. Rev. E* **72**, 046610 (2005); *Phys. Rev. E* **73**, 026601 (2006).
 - [32] D. Anderson, *Phys. Rev. A* **27**, 3135 (1983).
 - [33] Y. Cheng, *J. Phys. B: At. Mol. Opt. Phys.* **42** 205005, (2009).
 - [34] T. Gericke, P. Wurtz, D. Reitz, T. Langen and H. Ott, *Nat. Phys.* **4**, 949(2008).

